

# ANALYTICAL MODELLING OF LOW PRESSURE SINGLE BOSS SCULPTURED DIAPHRAGM AND ITS SENSITIVITY ENHANCEMENT

<sup>1</sup>D. Sindhanaiselvi, <sup>2</sup>R. Ananda Natarajan and <sup>3</sup>T. Shanmuganatham

<sup>1,2</sup>Department of Electronics and Instrumentation Engineering, Pondicherry Engineering College, India

E-mail: <sup>1</sup>sindhanaiselvi@pec.edu, <sup>2</sup>ananda\_natarajan@pec.edu

<sup>3</sup>Department of Electronics Engineering, Pondicherry University, India

E-mail: shanmuga.dee@pondiuni.edu.in

## Abstract

The low pressure is measured by using thin Sculptured diaphragm using micro system fabrication technology. The thickness of this diaphragm is reduced to improve sensitivity is achieved by boss like structure to increase the stiffness and reduce nonlinear deflection. This paper brings out the optimum design for single boss sculptured diaphragm. The burst pressure thickness is used to achieve the maximum possible sensitivity. The maximum stress regions identified for the proper placement of four polysilicon piezoresistors which are wired in the form of wheat stone bridge arrangement to estimate the electrical output. The results are obtained using Intellisuite MEMS CAD design tool. Mathematical modelling of single boss sculptured diaphragm results were compared with simulated results. Further the enhancement of sensitivity is analyzed using nonuniform thickness diaphragm and SOI technique. In this paper the low pressure analyzed in the range of (0-1000Pa). The simulation results indicate that the single boss square sculptured diaphragm with  $0.9\mu\text{m}$  yields the higher voltage sensitivity, acceptable linearity with Small Scale Deflection.

## Keywords:

Burst Pressure, Shape, Stress, Single Boss Sculptured Diaphragm, Nonuniform Thickness Diaphragm and SOI

## 1. INTRODUCTION

The acronym MEMS stands for micro electro mechanical systems and was coined in the United States in the late 1980s using micro systems technology. Today there are many companies working in the field of MEMS. MEMS based microsensors evident in everyday life continues to increase. This is due to advancement made in the development of Integrated Circuit (IC) fabrication process. This fabrication process reduced the size of sensor in addition it has added functionality and also the possibility of producing arrays of individual sensor elements on the same chip. Another feature that has influenced the popularity trend of microsensors is that many are based on silicon (Si) as it has excellent electrical and mechanical properties [7]. MEMS based micro devices find extensive application in different fields. Among all micro devices, MEMS pressure sensors are most popular both in industrial and commercial applications. In these devices, the diaphragm design is the major key part and it should be designed in such a way that it has high sensitivity with minimum thickness, acceptable linearity, physically realizable and does not break at the maximum pressure [17]. The piezoresistive type transduction mechanism, is used because it enables a linear operation over wide range of pressure and simple to fabricate [19]. Low pressure

sensing is possible only by thin diaphragms which lead to nonlinear deflection (balloon effect). This is reduced by using rigids or boss to increase the stiffness to limit the maximum deflection of the diaphragm [3] and resulting stress concentrated in relatively localized thin area [4].

The present authors have also focused their research on performance of sculptured diaphragm for low pressure application [22, 23]. In this paper, to enhance the sensitivity of sculptured diaphragm for low pressure application, a single boss with square and rectangular shape is analyzed with minimum thickness by burst pressure analysis [23]. The analytical modelling is obtained to validate the simulation results. Also, maximum stress concentration region is identified to place polysilicon piezoresistor [9] for improved voltage sensitivity with different placement pattern. In addition, the voltage sensitivity of this single boss sculptured diaphragm is enhanced by using nonuniform thickness and SOI technique is analyzed and compared with uniform thickness diaphragm.

## 2. MATERIALS AND METHODS

Typical single boss sculptured diaphragms is schematically shown in Fig.1.

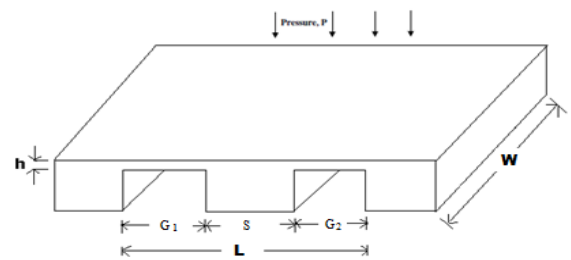


Fig.1. Cross Sectional View of the Single Boss Sculptured Diaphragm

The structure shown in Fig.1 are planar silicon diaphragm formed by bulk micromachining [10]. Single crystal silicon chosen because of its excellent mechanical and electrical properties and it is free of hysteresis and creep [14]. The polysilicon with suitable properties [12], [13], [15], [16] has been considered in this study to realize the piezoresistors using surface micromachining on the top of the diaphragm.

The sculptured diaphragm structures are simulated with the following material properties: Fracture strength: 7 GPa; Hardness: 850 Kg/mm<sup>2</sup>; Young's Modulus ( $E$ ): 170 GPa; Melting point: 1410°C; Gauge factor: 100 to 200; poisson's ratio ( $\nu$ ): 0.3. The dimensions for square and rectangular diaphragm considered [23] in this work are shown in Table.1.

Table.1. Dimensions of Diaphragm

Shape	L( $\mu\text{m}$ )	W( $\mu\text{m}$ )
Square	500	500
Rectangle	1000	500

### 3. MATHEMATICAL MODELLING

The diaphragm is designed with single rigid or support at the bottom in the center. The dimension of the diaphragm is ( $L\mu\text{m} \times W\mu\text{m} \times h\mu\text{m}$ )  $500\mu\text{m} \times 500\mu\text{m} \times 1\mu\text{m}$  where  $L$  is the length;  $W$  is the width and  $h$  is the thickness of the diaphragm respectively. The structure is created by bulk micromachining [10] with single crystal silicon by czochrolski process. The square and rectangular shapes are considered in this analysis because of the ease of fabrication by anisotropic wet chemical etching of silicon [18] wafers of  $\langle 100 \rangle$  orientation [5, 6] and larger sensitivity than circular diaphragms [11]. It is also easier to align the resistors parallel and perpendicular to the edges of the diaphragm which are in the  $\langle 110 \rangle$  direction, thus ensuring that the piezoresistive coefficients  $\pi_1$  and  $\pi_t$  are maximum along this direction.

The pressure-deflection model of a flat square diaphragm is given as,

$$\frac{Pa^4}{Eh^4} = \frac{4.2}{(1-\nu^2)} \left[ \frac{y}{h} \right] + \frac{1.58}{(1-\nu)} \left[ \frac{y}{h} \right]^3 \quad (1)$$

where,  $P$  is the applied pressure in  $Pa$ ,  $y$  is the center deflection of the diaphragm in  $\mu\text{m}$ ,  $a = L/2$  is the half side length of the diaphragm in  $\mu\text{m}$ ,  $E$  is the young's modulus in  $GPa$ ,  $h$  is the thickness of the diaphragm in  $\mu\text{m}$  and  $\nu$  is the poisson's ratio of the diaphragm material.

The first term in the RHS of Eq.(1) represents the Small Scale Deflection (SSD) that is very small compared with the diaphragm thickness (deflection is less than 40% of the diaphragm thickness), whereas the second term of Eq.(1) gives Large Scale Deflection (LSD), in which deflection is 40% larger than the diaphragm thickness [11].

To achieve Small Scale Deflection, the assumptions of thin plate deflection theory [2] considered are,

- The maximum membrane deflection is less than 40% of the membrane thickness.
- Membrane thickness doesnot exceed 10% of the diaphragm length.
- There is no initial stress in the membrane.

The deflection  $y$  in the linear region of operation with respect to thickness  $h$  is expressed as follows for a square diaphragm,

$$y = \frac{\alpha p L^4}{h^2 E} \quad \text{and} \quad \alpha = \frac{(1-\nu^2)}{4.2 \times 2^4} \text{ is a constant} \quad (2)$$

where,  $p$  is pressure applied,  $L$  is length of the diaphragm,  $h$  is thickness of the diaphragm,  $E$  is young's modulus and  $\alpha = 0.0138$  for  $L/W = 1$  (square). However, it cannot be used for characterizing the load deflection model of single sculptured diaphragms. Hence, it becomes necessary to develop a new model to describe the load deflection response of these sculptured diaphragms [21]. The Eq.(2) is suitably modified to describe the

equations for sculptured diaphragms. When the diaphragm is added with supports in the center, two important changes happen. First the active force loading area decreases. Second the rigidity of the diaphragm is reduced. So incorporating these factors in the modelling is essential to obtain the correct load deflection response. The side length  $L$  decides the loading area and the thickness ( $h$ ) of the diaphragm decides the rigidity in Eq.(2). Therefore, correctness or validity of the modified analytical model depends on the ability to define the effective side length  $L_{eff}$  and effective diaphragm thickness  $h_{eff}$  that replace  $L$  and  $h$  in Eq.(2). In sculptured diaphragm, one support of required dimension is added to a square diaphragm of  $500\mu\text{m} \times 500\mu\text{m}$  in the bottom which tends to change the effective  $L_{eff}$ . After the introduction of one support, the square diaphragm is modified into two rectangle diaphragm on the two sides of the support as shown in Fig.2 where the center displacement takes place on the centers of the two diaphragms as shown by the shaded regions.

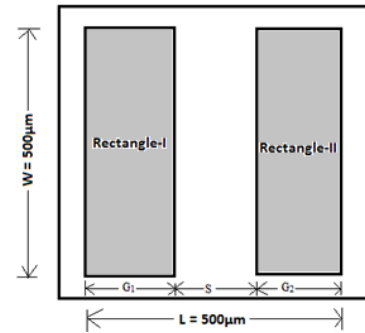


Fig.2. Top View of Single Boss Sculptured Diaphragm After Addition of Support

In the Fig.2,  $S$  is Support length ( $\mu\text{m}$ ),  $G_1$  is the length of new rectangle-I formed in the left side by addition of support ( $\mu\text{m}$ ) and  $G_2$  is the length of the new rectangle-II formed in the right side by addition of support ( $\mu\text{m}$ ),  $L$  - total length of the diaphragm and  $W$  - total width of diaphragm. Now the change in effective length on the two sides given in the following equation:

$$L_{eff} = \text{Total Length} - \text{Support Length} = L - S \quad (3)$$

Based on effective length,  $L_{eff}/W$  ratio, coefficients  $\alpha$  and  $\beta$  to be selected from the Table.2.

Table.2. Coefficients  $\alpha$ ,  $\beta_1$  and  $\beta_2$  with respect to  $L_{eff}/W$  ratio

$L_{eff}/W$	1	1.2	1.4	1.6	1.8	2.0	$\infty$
$\alpha$	0.0138	0.0188	0.0226	0.0251	0.0267	0.0277	0.0284
$\beta_1$	0.3078	0.3834	0.4356	0.4680	0.4872	0.4974	0.5000
$\beta_2$	0.1386	0.1794	0.2094	0.2286	0.2406	0.2472	0.25

Now the center deflection given by Eq.(2) is modified as,

$$y = \frac{\alpha P G_1^4}{E h^3} \quad (4)$$

where,  $G_1$  and  $G_2$  are the length of shaded region where maximum displacement occurs ( $\mu\text{m}$ ). Therefore  $G = G_1 = G_2$  ( $\mu\text{m}$ ). Similarly the effective diaphragm thickness  $h_{eff}$  obtained from the new

structure after addition of support can be written as given in the following equation,

$$h_{eff} = h. \quad (5)$$

As there is no change in the thickness, it remains the same. Now the modified displacement equation for the diaphragm with support can be written as given in the following equation,

$$y = \frac{\alpha P G^4}{E h^3} \quad (6)$$

The stress developed in the YY and XX direction in the diaphragm under different applied pressure in the SSD region is given by the Eq.(7),

$$\sigma_{yy} = \beta_1 P \left[ \frac{G}{h} \right]^2 \quad \text{and} \quad \sigma_{xx} = \beta_2 P \left[ \frac{G}{h} \right]^2 \quad (7)$$

where,  $P$  is pressure applied in  $Pa$ ,  $G$  is length of the new rectangle in  $\mu m$  and  $h$  is thickness of diaphragm in  $\mu m$ .

The equation for the wheatstone bridge output voltage ( $V_o$ ) is given as,

$$\frac{V_o}{V_b} = \frac{R_4}{R_4 + R_1} - \frac{R_3}{R_2 + R_3} \quad (8)$$

where,  $V_b$  is bridge excitation voltage. Initially resistance  $R_1 = R_2 = R_3 = R_4 = R_o$  which is the resistance at zero pressure. When pressure is applied, change in resistance with respect to  $R_o$  is changed as follows,

$$\frac{\Delta R}{R_o} = \frac{(\pi_{11} + \pi_{12} + \pi_{44})\sigma_l + (\pi_{11} + \pi_{12} - \pi_{44})\sigma_t}{2} \quad (9)$$

where,  $\sigma_l$  and  $\sigma_t$  are the longitudinal and tensile stress along the diaphragm. In longitudinal orientation, for  $R_2$  and  $R_4$ :  $\sigma_l = \sigma_1$ MPa and  $\sigma_t = \sigma_2$  MPa. In transverse orientation, for  $R_1$  and  $R_3$ :  $\sigma_l = \sigma_2$ MPa and  $\sigma_t = \sigma_1$ MPa.

When pressure applied, the new change in resistance are obtained by the following equations,

$$R_1 = R_3 = R_o(1 + 0.5 \times (1.436 \times \sigma_l - 1.326 \times \sigma_t) \times 10^{-3}) \quad (10)$$

$$R_2 = R_4 = R_o(1 + 0.5 \times (1.436 \times \sigma_l - 1.326 \times \sigma_t) \times 10^{-3}) \quad (11)$$

where,  $R_2$  and  $R_4$  are in longitudinal direction and  $R_1$  and  $R_3$  are in transverse direction. Substituting Eq.(10) and Eq.(11) in Eq.(8), the voltage sensitivity is obtained as in Eq.(12),

$$\frac{V_o}{V_b} = \frac{2.762 \times 10^{-3} (\sigma_l - \sigma_t)}{4 + 0.11 \times 10^{-3} (\sigma_l + \sigma_t)} \quad (12)$$

## 4. ANALYSIS FOR OPTIMIZED DESIGN IN THE LOW PRESSURE RANGE

### 4.1. DIAPHRAGM GEOMETRY DESIGN OPTIMIZATION

The single boss sculptured diaphragm created has three regions at the bottom of the substrate namely  $G_1$ ,  $G_2$  and  $S$  as in Fig.1. The main objective of this section is to analyze the positioning of the boss by varying these regions to achieve the maximum deflection sensitivity within the small scale deflection region for square and rectangular diaphragms. The sensor is subjected to pressure on the front side as in Fig.1, where the

piezoresistors are to be placed. The pressure range varied from 0 to 1000 Pa. The thickness of the sculptured diaphragm is reduced to increase the stress concentration as in Eq.(7). This reduced thickness for the square and rectangular sculptured diaphragm is obtained from burst pressure characteristics as in [23]. Burst pressure  $P_B$  is defined as the pressure at which maximum stress  $\sigma_{max}$  on the diaphragm becomes equal to the critical stress  $\sigma_c$  which is actually the yield strength of material [17], [18], [19], [20]. So during optimization, the thickness of the sculptured diaphragm is selected in between  $0.5\mu m$  to  $1\mu m$  to avoid burst condition [23]. The optimized dimension of single boss sculptured diaphragm with thickness, center deflection and percentage of center deflection were given in Table.3.

Table.3. Optimized Dimension

Shape	$h$ ( $\mu m$ )	$G_1$ ( $\mu m$ )	$G_2$ ( $\mu m$ )	$S$ ( $\mu m$ )	$y$ ( $\mu m$ )	$y_p$ (%)
Square	0.9	170	170	160	0.1525	17
Rectangle	1	180	180	640	0.1892	18

where,  $h$  - Thickness,  $G_1$ ,  $G_2$  - Support gap width,  $S$  - Support width,  $y$  - Center deflection and  $y_p$  - Percentage of center deflection with respect to thickness. The percentage of center deflection shows that it satisfies the small scale deflection which is less than 20% and the thickness is less than 10% of diaphragm length. The square sculptured diaphragm is optimized with thickness  $0.9\mu m$  and rectangular sculptured diaphragm with thickness  $1\mu m$ .

The center deflection of simulated single boss sculptured diaphragm of square type is shown in Fig.3.

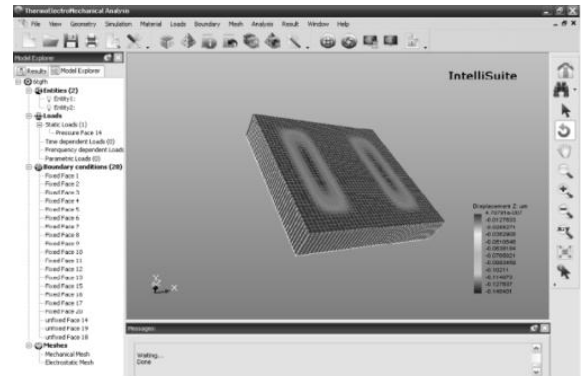


Fig.3. Simulated Single Boss Sculptured Diaphragm with Center Deflection – Square Type

The maximum deflection regions are highlighted in blue colour which occurs in the center of two shaded rectangle region as referred in Fig.2. The center deflection of rectangle type single boss sculptured is also similar and occur in the center of the two shaded rectangle regions.

### 4.2 STRESS AND PIEZORESISTIVE ANALYSIS

The maximum longitudinal and transverse stress regions estimated at 1000Pa for the optimized single boss diaphragm of square type from the previous section were analyzed and shown in Fig.4 and Fig.5.

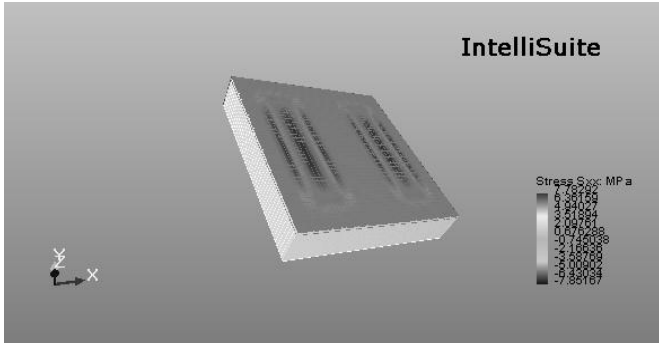


Fig.4. Maximum Longitudinal Stress Distribution

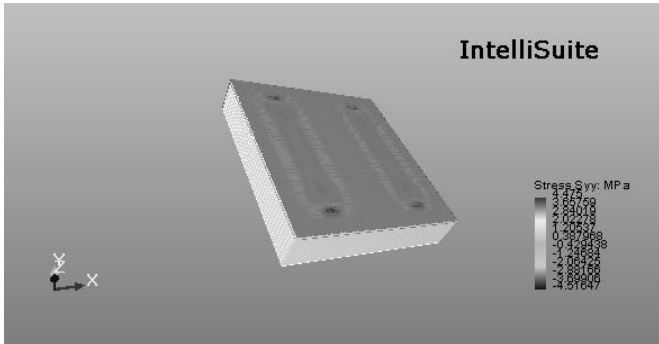


Fig.5. Maximum Transverse Stress Distribution

The Fig.4 shows that, the maximum longitudinal stress  $S_{xx}$  (highlighted red) occurs at  $(90\mu\text{m}, 250\mu\text{m})$  and  $(160\mu\text{m}, 250\mu\text{m})$  from the center of the diaphragm in the vertical direction. Similarly, Fig.5 shows that the maximum transverse stress  $S_{yy}$  occurs (highlighted red) at  $(170\mu\text{m}, 250\mu\text{m})$  in the horizontal direction. The stress simulation result of rectangular type is also similar but reveals a decrease in  $S_{xx}$  value and increase in  $S_{yy}$  value compared with square type as in Table.5.

To improve the voltage sensitivity, the four resistors are to be placed in such a way that two resistors ( $R_1, R_3$ ) experience tensile stress and exhibit increase in their resistance and the remaining two resistors ( $R_2, R_4$ ) experience compressive stress and exhibit decrease in their resistance from the resistance value measured at no stress condition. Hence to achieve this, the arrangement of resistors is estimated in four different categories as shown in Fig.6.

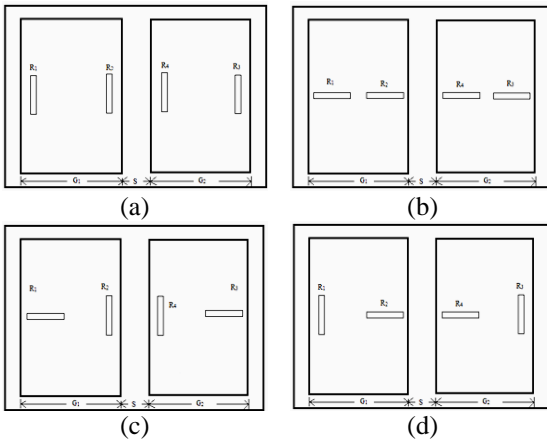


Fig.6. Different Arrangement of Piezoresistors Placement

The comparisons of the estimated output voltage with respect to placement patterns of the piezoresistor were given in Table.4. Polysilicon piezoresistors ( $R_1, R_2, R_3$  and  $R_4$ ) are used in the maximum stress regions identified on the diaphragm [9] with smith piezoresistive coefficients [1] are as follows:  $\pi_{11} = 6.6 \times 10^{-11} \text{Pa}^{-1}$ ;  $\pi_{12} = -1.1 \times 10^{-11} \text{Pa}^{-1}$ ;  $\pi_{44} = 138 \times 10^{-11} \text{Pa}^{-1}$ . The dimensions of the piezoresistor used were  $16\mu\text{m} \times 2\mu\text{m} \times 1\mu\text{m}$ . The sheet resistance of p-type silicon resistor is  $25\Omega/\text{square.cm}$  and temperature =  $20^\circ\text{C}$ .

Table.4. Voltage Output versus Different Placement Pattern

Placement Pattern	Output Voltage (V)
a	$86\mu\text{V}$
b	$50\mu\text{V}$
c	$1.4\text{mV}$
d	<b><math>2.4\text{mV}</math></b>

Among the four patterns shown in Fig.6, pattern (d) gives highest voltage sensitivity of  $2.4\text{mV}$  at  $1000\text{Pa}$ . It reveals that, pattern (d) is suitable and efficient in extracting the maximum stress into maximum change in resistance which in turn gives the higher voltage sensitivity.

### 4.3 ELECTRICAL OUTPUT

The four polysilicon piezoresistors are wired in the form of wheat stone bridge assembly to estimate the electrical output with the supply voltage of  $5\text{V}$  [23]. The four piezoresistor are chosen to achieve better temperature compensation. The longitudinal stress, transverse stress and electrical output for two cases of single boss sculptured diaphragm were compared in Table.5 at a maximum pressure of  $1000\text{Pa}$ .

Table.5. Comparison of Center Deflection, Longitudinal Stress, Transverse Stress and Electrical Output with Simulated and Analytical Output

Results	Thickness $h$ ( $\mu\text{m}$ )	Diaphragm Shape $L \times W$ ( $\mu\text{m}$ )	Center Deflection ( $\mu\text{m}$ )	Deflection $y_p$ in %	Longitudinal Stress $S_{xx}$ (MPa)	Transverse Stress $S_{yy}$ (MPa)	$V_o$ (mV)
Simulated	0.9	Square $500 \times 500$	0.1525	17	7.783	4.475	2.283
	1	Rectangle $1000 \times 500$	0.1892	18	7.279	5.150	1.469
Analytical	0.9	Square $500 \times 500$	0.1672	18.5	8.168	4.709	2.386
	1	Rectangle $1000 \times 500$	0.1901	19	7.576	5.351	1.536

The comparison of simulated and analytical results shows that 4.7% measurement error which indicates the lack of material property. On comparing the deflection  $y_p$  in % and output voltage from Table.5, the single boss sculptured diaphragm with square yields small scale deflection sensitivity and voltage sensitivity

than rectangle boss sculptured diaphragm.

On comparing shapes, square sculptured diaphragm needs smaller thickness to sense low pressure ranges than the rectangle sculptured diaphragm to yield good voltage sensitivity.

On comparing stress values, square diaphragm yields higher longitudinal stress than rectangular diaphragm. But the transverse stress is higher for rectangular diaphragm than square type. In addition, it is also found that the longitudinal stress of square type is 7.783MPa and rectangle type is 7.279MPa. Similarly the transverse stress of square type is 4.475MPa and rectangle type is 5.150MPa. The stress values were almost equal for square and rectangular diaphragm.

**4.4 ENHANCEMENT OF SENSITIVITY**

The stress obtained from the previous section is improved by incorporating the size of piezoresistor, modifying the thickness of diaphragm and diaphragm with SOI. The output voltage is estimated with respect to different piezoresistor size using placement pattern (d) from Fig.6 and compared in Table.6.

Table.6. Piezoresistor Size versus Output Voltage

Piezoresistor Size	Output Voltage
40µm×20µm×1µm	160µV
20µm×10µm×1µm	300µV
<b>16µm×2µm×1µm</b>	<b>2.13mV</b>
10µm×5µm×0.5µm	3.0mV

The results obtained shows that small size 10µm×5µm×0.5µm of piezoresistors gives the maximum sensitivity when compared with large size piezoresistors. But for the ease of fabrication, **16µm×2µm×1µm** is chosen to estimate the output voltage in the next section.

The single boss sculptured diaphragms constructed with uniform thickness shows that the maximum stress are almost close to each other for all types of diaphragm. In order to maximize and concentrate the stress in the supported region to improve the sensitivity, now the total thickness is divided into two values as ‘h’ and ‘h<sub>1</sub>’ where ‘h’ is the uniform thickness and ‘h<sub>1</sub>’ is the thickness which is added only in the support regions which in turn increase the stress value. The new proposed structure for single boss sculptured diaphragm is shown in Fig.7.

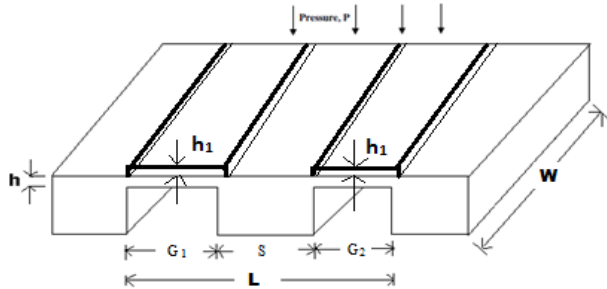


Fig.7. Cross Sectional View of Single Boss Sculptured Diaphragm with Non Uniform Thickness

The single support square sculptured diaphragm with non-uniform thickness created and their estimated output presented in Table.7.

Table.7. Comparison of Center Deflection, Longitudinal Stress, Transverse Stress and Electrical Output of Single Boss Sculptured Diaphragm – Square

Thickness (µm) <i>h = h + h<sub>1</sub></i>		Center Deflection (µm)	Percentage of Center deflection <i>y<sub>p</sub></i> (%)	<i>S<sub>xx</sub></i> (MPa)	<i>S<sub>yy</sub></i> (MPa)	<i>V<sub>o</sub></i> (mV/Pa)
<i>h = 0.1</i>	<i>h<sub>1</sub> = 0.5</i>	0.4744	74	25.96	10.465	10.69
<i>h = 0.2</i>	<i>h<sub>1</sub> = 0.5</i>	0.3002	42	19.1	7.5393	7.979
<b><i>h = 0.3</i></b>	<b><i>h<sub>1</sub> = 0.5</i></b>	<b>0.2022</b>	<b>22</b>	<b>14.59</b>	<b>5.8165</b>	<b>6.051</b>

The single support rectangle sculptured diaphragm with non-uniform thickness created and their estimated output presented in Table.8.

Table.8. Comparison of Center Deflection, Longitudinal Stress, Transverse Stress and Electrical Output of Single Boss Sculptured Diaphragm – Rectangle

Thickness (µm) <i>h = h + h<sub>1</sub></i>		Center Deflection (µm)	Percentage of Center deflection <i>y<sub>p</sub></i> (%)	<i>S<sub>xx</sub></i> (MPa)	<i>S<sub>yy</sub></i> (MPa)	<i>V<sub>o</sub></i> (mV/Pa)
<i>h = 0.3</i>	<i>h<sub>1</sub> = 0.5</i>	0.3437	42	16.38	8.2224	5.629
<i>h = 0.4</i>	<i>h<sub>1</sub> = 0.5</i>	0.2422	27	12.89	6.5	4.413
<b><i>h = 0.5</i></b>	<b><i>h<sub>1</sub> = 0.5</i></b>	<b>0.1773</b>	<b>17</b>	<b>10.39</b>	<b>5.2629</b>	<b>3.544</b>

The center deflection within 40% is considered within small scale deflection to ensure linearity. From the results obtained, single boss square with 22% deflection and output 6.051mV is optimized.

Similarly, for the single boss rectangle with 27% deflection and output 4.413mV is optimized. The result shows that the modified thickness by stiffening the sculptured regions improved the stress from lower value to higher value and sensitivity is increased.

The sensitivity is further enhanced by using SOI structure [8], [17], [20] is created using the surface micromachining technique. The SOI MEMS pressure sensor structure for single sculptured diaphragm is shown in Fig.8.

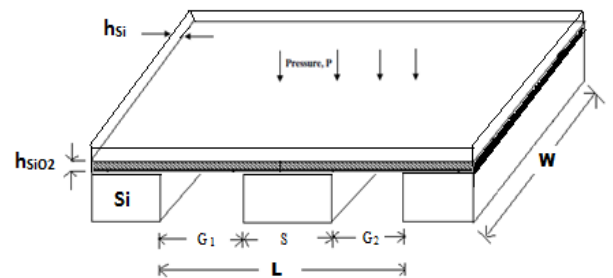


Fig.8. Single Sculptured Diaphragm with SOI

The sculptured diaphragm with SOI is created and its comparison of the improved longitudinal stress, transverse stress, center deflection, percentage of center deflection and voltage

output were estimated for square and rectangle diaphragm is given in Table.9 and Table.10.

Table.9. Comparison of Center Deflection, Longitudinal Stress, Transverse Stress and Electrical Output of Single Boss Sculptured Diaphragm with SOI – Square

Thickness ( $\mu\text{m}$ ) $h=h+h_1$		Center Deflection ( $\mu\text{m}$ )	Percentage of Center deflection $y_p$ (%)	$S_{xx}$ (MPa)	$S_{yy}$ (MPa)	$V_o$ (mV/Pa)
$h_{Si} = 0.2$	$h_{SiO_2} = 0.6$	0.334	40	12.37	4.9994	5.08
$h_{Si} = 0.15$	$h_{SiO_2} = 0.6$	0.362	45	13.2	5.3369	5.428

The single square sculptured diaphragm with SOI yield the higher sensitivity of 5.08mV and small scale deflection is 40% with silicon diaphragm thickness 0.2 $\mu\text{m}$ . The other case yields 5.428mV but deflection is 45% not satisfying SSD with silicon diaphragm thickness 0.15 $\mu\text{m}$ .

Table.10. Comparison of Center Deflection, Longitudinal Stress, Transverse Stress and Electrical Output of Single Boss Sculptured Diaphragm with SOI – Rectangle

Thickness ( $\mu\text{m}$ ) $h=h+h_1$		Center Deflection ( $\mu\text{m}$ )	Percentage of Center deflection $y_p$ (%)	$S_{xx}$ (MPa)	$S_{yy}$ (MPa)	$V_o$ (mV/Pa)
$h_{Si} = 0.2$	$h_{SiO_2} = 0.6$	0.5703	70	15.44	6.749	6.001
$h_{Si} = 0.3$	$h_{SiO_2} = 0.6$	0.3963	42	11.77	5.377	4.411

The single boss rectangle sculptured diaphragm with SOI yield the higher sensitivity of 4.411mV with 42% deflection and 6mV with 70% deflection. The 42% deflection is closer to small scale deflection with 4.4mV is optimized output using SOI layer to improve sensitivity.

#### 4.5 COMPARISON OF SENSITIVITY FOR PROPOSED METHODS

The single boss sculptured diaphragms of square and rectangle shape were created and their output for the pressure in range of 0-1000Pa are compared and analyzed for different proposed methods.

The three proposed cases were uniform thickness of diaphragm, non-uniform thickness of diaphragm and SOI thickness diaphragm. The measured electrical outputs of square and rectangular with single boss sculptured diaphragm were compared in terms of its sensitivity is shown in Fig.9 and Fig.10.

The output obtained for square diaphragm in Fig.9 shows that the non-uniform thickness technique yields higher sensitivity of 6.05mV than the other proposed methods. The uniform thickness technique yields 2.386mV and SOI technique yields 5.08mV at 1000Pa.

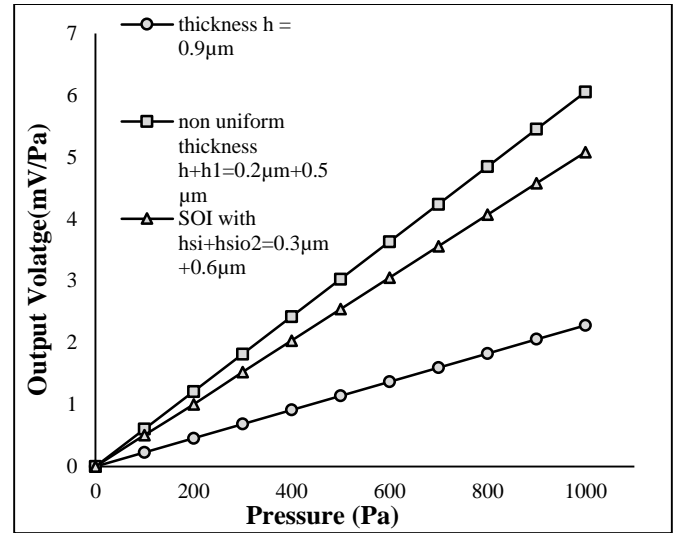


Fig.9. Comparison of Applied Pressure versus Electrical Output of Square Sculptured Diaphragm for Different Proposed Methods

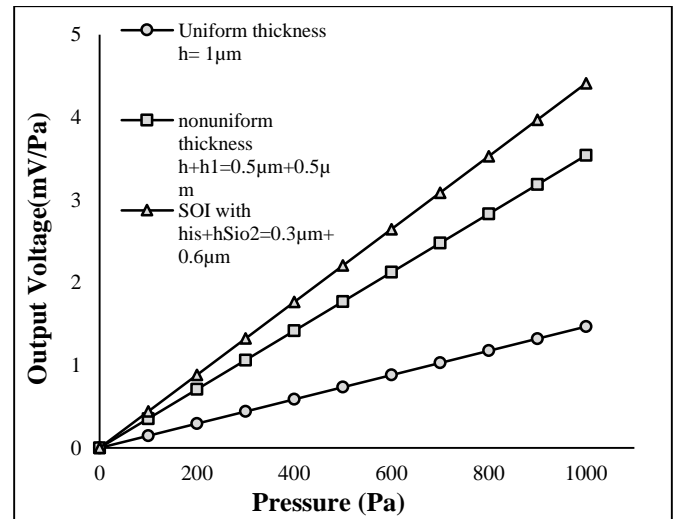


Fig.10. Comparison of Applied Pressure versus Electrical Output of Rectangle Sculptured Diaphragm for Different Proposed Methods

Similarly, the output obtained for rectangular diaphragm in Fig.10 shows that the single boss sculptured diaphragm with SOI technique yields higher sensitivity of 4.41mV with 42% deflection. The non-uniform thickness technique yields 3.5mV with 17% deflection and uniform thickness yields 1.469mV at 1000Pa.

#### 5. CONCLUSION

The feasibility of achieving greater sensitivity with reasonably good linearity with sculptured diaphragms using smaller thickness was investigated. The effects of single boss with square and rectangular shape on the displacement, stress and voltage sensitivity have been analyzed using Intellisuite MEMS CAD tool. The comparison of single boss diaphragm result shows that the square diaphragm yields higher voltage sensitivity than the rectangular diaphragm using smaller thickness. The analytical modelling for single boss sculptured diaphragm obtained and

validated with the simulation results. The better sensitivity is achieved by analyzing different placement pattern of piezoresistor and size of piezoresistor is attempted. Further, sensitivity is enhanced by using non-uniform thickness technique and SOI technique. The non-uniform thickness technique reveals that it is possible to enhance stress to a higher value from 7.78MPa to 14.59MPa which also satisfies small scale deflection. The sensitivity of uniform thickness diaphragm with 2.283mV is improved to 5.08mV for SOI technique and 6.051mV for non-uniform thickness technique using square diaphragm.

## ACKNOWLEDGEMENT

The authors express their sincere gratitude to Dr. R. Joseph Daniel for his encouragement and useful discussions. The authors gratefully acknowledge the support from authorities of National Program on Micro and Smart Systems (NPMAS) Centre of Annamalai University interns of MEMS software design tools.

## REFERENCES

- [1] Charles S. Smith, "Piezoresistance Effect in Germanium and Silicon", *Physical Review Letters*, Vol. 94, No. 1, pp. 42-49, 1954.
- [2] S. Timoshenko and S. Woinowsky-Krieger, "*Theory of Plates and Shells*", McGraw-Hill, 1959.
- [3] Joseph R. Mallon, Farzad Pourahmadi, Kurt Petersen, Phillip Barth, Ted Vermeulen and Janusz Brezek, "Low Pressure Sensors Employing Bossed Diaphragms and Precision Etch Stopping", *Sensors and Actuators A: Physical*, Vol. 21, No. 1-3, pp. 89-95, 1990.
- [4] H. Sandmaier, "Non-Linear Analytical Modeling of Bossed Diaphragms for Pressure Sensors", *Sensors and Actuators A: Physical*, Vol. 25, No. 1-3, pp. 815-819, 1991.
- [5] Yozo Kanda and Aiko Yasukawa, "Optimum Design Considerations for Silicon Piezoresistive Pressure Sensors", *Sensors and Actuators A: Physical*, Vol. 62, No. 1-3, pp. 539-542, 1997.
- [6] Liwei Lin and Weijie Yun, "Design, Optimization & Fabrication of Surface Micromachined Pressure Sensors", *Journal of Mechatronics*, Vol. 8, No. 5, pp. 505-519, 1998.
- [7] Stephen P. Beeby, Graham Ensel and Michael Kraft, "*MEMS Mechanical Sensors*", Artech House, 2004.
- [8] P.D. Dimitropoulos, C. Kachris, D.P. Karampatzakisa and G.I. Stamoulis, "A New SOI Monolithic Capacitive Sensor for Absolute and Differential Pressure Measurements", *Sensors and Actuators A: Physical*, Vol. 123-124, pp. 36-43, 2005.
- [9] K. Sivakumar, N. Dasgupta, K.N. Bhat and K. Natarajan, "Sensitivity Enhancement of Polysilicon Piezoresistive Pressure Sensors with Phosphorous Diffused Resistors", *Journal of Physics: Conference series*, Vol. 34, No. 1, pp. 216-221, 2006.
- [10] Xiaodong Wang, Baoqing Li, Onofrio L. Russo, Harry T. Roman, Ken K. Chin and Kenneth R. Farmer, "Diaphragm Design Guidelines and an Optical Pressure Sensor Based on MEMS Technique", *Microelectronics Journal*, Vol. 37, No. 1, pp. 50-56, 2006.
- [11] Zhao Linlin, Xu Chen and Shen Guangdi, "Analysis for Load Limitations of Square-Shaped Silicon Diaphragms", *Solid State Electronics*, Vol. 50, No. 9-10, pp. 1579-1583, 2006.
- [12] A. Wisitorsaat, V. Patthanasetakul, T. Lomas and Tuantranont, "Low Cost Thin Film Based Piezoresistive MEMS Tactile Sensor", *Sensors and Actuators A: Physical*, Vol. 139, No. 1-2, pp. 17-22, 2007.
- [13] Ingelin Clausen and Ola Svein, "Die Separation and Packaging of a Surface Micromachined Piezoresistive Pressure Sensor", *Sensors and Actuators A: Physical*, Vol. 133, No. 2, pp. 457-466, 2007.
- [14] K.N. Bhat, "Silicon Micromachined Pressure Sensors", *Journal of the Indian Institute of Science*, Vol. 87, No.1, pp. 115-131, 2007.
- [15] Shyam Aravamudhan and Shekhar Bhansali, "Reinforced Piezoresistive Pressure Sensor for Ocean Depth Measurements", *Sensors and Actuators A: Physical*, Vol. 142, No 1, pp. 111-117, 2008.
- [16] Milon M. Jevti and Miloljub A. Smiliani, "Diagnostic of Silicon Piezoresistive Pressure Sensors by Low Frequency Noise Measurements", *Sensors and Actuators A: Physical*, Vol. 144, No. 2, pp. 267-274, 2008.
- [17] M. Narayanaswamy, R. Joseph Daniel, K. Sumangala and C. Antony Jeyasehar, "Computer Aided Modelling and Diaphragm Design Approach for High Sensitivity Silicon-On-Insulator Pressure Sensors", *Measurement*, Vol. 44, No. 10, pp. 1924-1936, 2011.
- [18] Vidhya Balaji and K.N. Bhat, "A Comparison of Burst Strength and Linearity of Pressure Sensors Having Thin Diaphragms of Different Shapes", *Journal of Institute of Smart Structures And Systems*, Vol. 2, No. 2, pp. 18-26, 2012.
- [19] K.N. Bhat and M.M. Nayak, "MEMS Pressure Sensors—An Overview of Challenges in Technology and Packaging", *Journal of Institute of Smart Structures and Systems*, Vol. 2, No. 1, pp. 39-71, 2013.
- [20] M. Narayanaswamy, R. Joseph Daniel and K. Sumangala, "Piezoresistor Size and Placement Effect on Sensitivity of Silicon-On-Insulator Piezoresistive Pressure Sensor", *Journal of Instrument Society of India*, Vol. 43, No. 3, pp. 208-211, 2013.
- [21] M. Rajavelu, D. Sivakumar, R. Joseph Daniel and K. Sumangala, "Perforated Diaphragms Employed Piezoresistive MEMS Pressure Sensor for Sensitivity Enhancement in Gas Flow Measurement", *Flow Measurement and Instrumentation*, Vol. 35, pp. 63-75, 2014.
- [22] D. Sindhanaiselvi, R. Ananda Natarajan and T. Shanmuganatham, "Performance Analysis of Sculptured Diaphragm for Low Pressure MEMS Sensors", *Applied Mechanics and Materials*, Vol. 592-594, pp. 2193-2198, 2014.
- [23] D. Sindhanaiselvi, R. Ananda Natarajan and T. Shanmuganatham, "Design and Optimization of Low Pressure Sculptured Diaphragm with Burst Pressure, Stress Analysis and its Enhancement", *International Journal of Applied Engineering Research*, Vol. 10, No.24, pp. 21075-21081, 2015.

